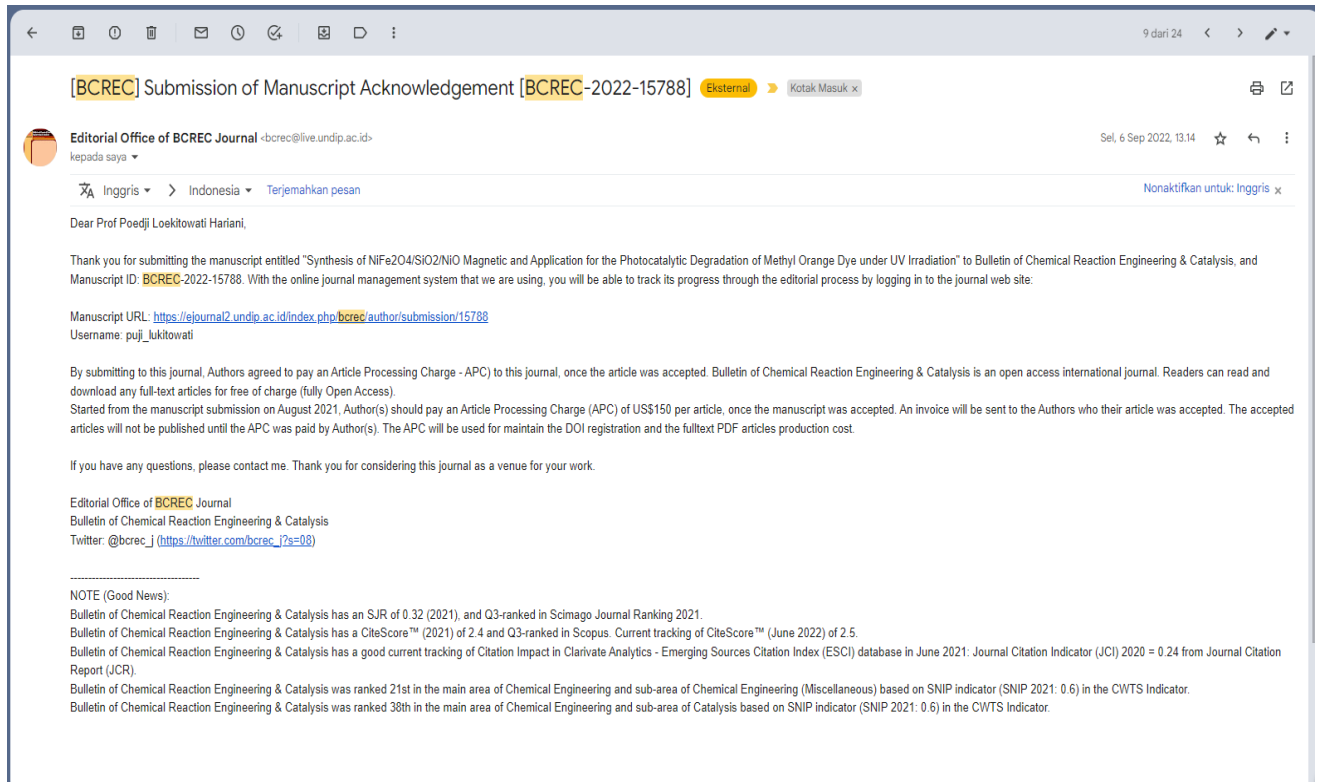


Korespondensi Bulletin of Chemical Reaction Engineering & Catalysis, Vol 17, No 4, 2022

Judul artikel: Synthesis of NiFe₂O₄/SiO₂/NiO Magnetic and Application for the Photocatalytic Degradation of Methyl Orange Dye under UV Irradiation

Author: Poedji Loekitowati Hariani, Muhammad Said, Addy Rachmat, Salni, Nabila Aprianti, Anisa Fitri Amatullah



9 dari 24 < > ✎

[BCREC] Submission of Manuscript Acknowledgement [BCREC-2022-15788] Eksternal > Kotak Masuk x

Editorial Office of BCREC Journal <bcrec@live.undip.ac.id> kepada saya ▾ Sel, 6 Sep 2022, 13.14 ☆ ↶ ⋮

🌐 Inggris ▾ > Indonesia ▾ Terjemahkan pesan Nonaktifkan untuk: Inggris x

Dear Prof Poedji Loekitowati Hariani,

Thank you for submitting the manuscript entitled "Synthesis of NiFe₂O₄/SiO₂/NiO Magnetic and Application for the Photocatalytic Degradation of Methyl Orange Dye under UV Irradiation" to Bulletin of Chemical Reaction Engineering & Catalysis, and Manuscript ID: BCREC-2022-15788. With the online journal management system that we are using, you will be able to track its progress through the editorial process by logging in to the journal web site:

Manuscript URL: <https://ejournal2.undip.ac.id/index.php/bcrec/author/submission/15788>
Username: puji_lokitowati

By submitting to this journal, Authors agreed to pay an Article Processing Charge - APC) to this journal, once the article was accepted. Bulletin of Chemical Reaction Engineering & Catalysis is an open access international journal. Readers can read and download any full-text articles for free of charge (fully Open Access). Started from the manuscript submission on August 2021, Author(s) should pay an Article Processing Charge (APC) of US\$150 per article, once the manuscript was accepted. An invoice will be sent to the Authors who their article was accepted. The accepted articles will not be published until the APC was paid by Author(s). The APC will be used for maintain the DOI registration and the fulltext PDF articles production cost.

If you have any questions, please contact me. Thank you for considering this journal as a venue for your work.

Editorial Office of BCREC Journal
Bulletin of Chemical Reaction Engineering & Catalysis
Twitter: @bcrec_j (https://twitter.com/bcrec_j?s=08)

NOTE (Good News):
Bulletin of Chemical Reaction Engineering & Catalysis has an SJR of 0.32 (2021), and Q3-ranked in Scimago Journal Ranking 2021.
Bulletin of Chemical Reaction Engineering & Catalysis has a CiteScore™ (2021) of 2.4 and Q3-ranked in Scopus. Current tracking of CiteScore™ (June 2022) of 2.5.
Bulletin of Chemical Reaction Engineering & Catalysis has a good current tracking of Citation Impact in Clarivate Analytics - Emerging Sources Citation Index (ESCI) database in June 2021: Journal Citation Indicator (JCI) 2020 = 0.24 from Journal Citation Report (JCR).
Bulletin of Chemical Reaction Engineering & Catalysis was ranked 21st in the main area of Chemical Engineering and sub-area of Chemical Engineering (Miscellaneous) based on SNIP indicator (SNIP 2021: 0.6) in the CWTS Indicator.
Bulletin of Chemical Reaction Engineering & Catalysis was ranked 38th in the main area of Chemical Engineering and sub-area of Catalysis based on SNIP indicator (SNIP 2021: 0.6) in the CWTS Indicator.

8 dari 24

Prof. Dr. Istadi Istadi <bcrec@live.undip.ac.id>
kepada saya, Muhammad, Addy, Sahni, Nabila, Anisa

Rab, 21 Sep 2022, 06.05

Inggris > Indonesia > Terjemahkan pesan Nonaktifkan untuk: Inggris x

Journal Name: Bulletin of Chemical Reaction Engineering & Catalysis
Article Title: Synthesis of NiFe₂O₄/SiO₂/NiO Magnetic and Application for the Photocatalytic Degradation of Methyl Orange Dye under UV Irradiation
Ms-ID: BCREC-2022-15788

Dear Prof Poedji Loekitowati Hariani,

Reviewers have now commented on your paper (attached below this email). You will see that they are advising that you must revise your manuscript accordingly. If you are prepared to undertake the work required, I would be pleased to reconsider my decision. Authors are encouraged to respond to all Reviewers' comments.
For your guidance, reviewers' comments can be read in your Author online interface. If you decide to revise the work, please submit a list of changes or a rebuttal against each point which is being raised when you submit the revised manuscript.

****>>>Please be noted that you have up to 1 (one) months from now to revise your manuscript, unless your manuscript will be considered as a new submitted manuscript. NOTE: If you need additional time to complete your revision, please let us know by replying to this email and informing us of the date you expect to submit it. <<<<****

To submit a revision, please upload your revised manuscript documents to BCREC online submission interface at (<https://ejournal2.undip.ac.id/index.php/bcrec>) after you login as Author. Important: Please indicate the revision as blue-highlighting the revision sentences or words within your revised manuscript.

To upload your revised document files (three files), the following MUST be included:

- One (1) file of "Revision Note" file in a table form with respect to Reviewers comments including the location of the revision on the revised manuscript. Template MS Word File of this Revision Note can be downloaded here: <https://bit.ly/3cvzcS8>
- One (1) file of "Revised Manuscript" file according to Template-based format (MS Word file) (please blue-color highlighted texts in the revised sentences).
- One (1) file of "Graphical Abstract" file according to Guideline of Graphical Abstract (<https://ejournal2.undip.ac.id/index.php/bcrec/pages/view/graphicalabstract/>).

GUIDELINE TO UPLOAD REVISION: To upload your revised manuscript, please login to BCREC journal submission interface (<https://ejournal2.undip.ac.id/index.php/bcrec>) then login using your user and password as usual. Therefore, click on "Active" and click on the title of your manuscript. Under the header of "#xxxx Summary" there are three taskbars, i.e. "Summary", "Review", "Editing" and click on "Review". In the section of Editor Decision, please upload your revised manuscript file within sub section of "Upload Author Version", please just browse the file, and click on "Upload".
For second and continuing order of revision of manuscript, please just add your latest version file(s), do not delete the previous round of file(s) of manuscript.

IMPORTANT NOTE: A GRAPHICAL ABSTRACT of each article is mandatory for this journal. Please read detail guidelines here: <https://ejournal2.undip.ac.id/index.php/bcrec/pages/view/graphicalabstract/>
This graphic should capture the reader's attention and, in conjunction with the manuscript title, should give the reader a quick visual impression of the essence of the manuscript without providing specific results.
Choosing/Creating a Graphical Abstract: The graphic should be simple, but informative. The use of color is encouraged; The graphic should uphold the standards of a scholarly, professional publication. The graphic must be entirely original, unpublished artwork created by one of the coauthors; The graphic should not include a photograph, drawing, or caricature of any person, living or deceased; Do not include postage stamps or currency from any country, or trademarked items (company logos, images, and products); Avoid choosing a graphic that already appears within the text of the manuscript. Image size: please provide an image with a size of 500 x 800 pixels (height x width). Preferred file types: TIFF, JPG, PNG, PDF, or MS Office files.

The Graphical Abstracts should be submitted as a separate file during the revised manuscript submission system or otherwise, it can be submitted by email to: bcrec@live.undip.ac.id

2 dari 24

Pre publishing your article (BCREC-2022-15788) in Bulletin of Chemical Reaction Engineering & Catalysis Volume 17 Issue 4 Year 2022 (Issue in Progress) Eksternal Kotak Masuk x

BCREC Group <bcrec@live.undip.ac.id>
kepada saya

Jum, 7 Okt 2022, 15.31

Inggris > Indonesia > Terjemahkan pesan Nonaktifkan untuk: Inggris x

Dear Authors,

The Editorial Office of BCREC has just finalized your article (BCREC-2022-15788) entitled: "Synthesis of NiFe₂O₄/SiO₂/NiO Magnetic and Application for the Photocatalytic Degradation of Methyl Orange Dye under UV Irradiation".

The Editorial Office of BCREC journal notified you about pre-publishing your article (BCREC-2022-15788) in Bulletin of Chemical Reaction Engineering & Catalysis Volume 17 Issue 4 Year 2022 (Issue in Progress), pages 699-711, here in the issue: <https://ejournal2.undip.ac.id/index.php/bcrec/issue/view/1024> or you can directly access your article using the following DOI number of the article: <https://doi.org/10.9767/bcrec.17.4.15788.699-711>

Thank you for your contribution to this journal.

Best regards

Editorial Office
Bulletin of Chemical Reaction Engineering & Catalysis (ISSN 1978-2993)
Website of BCREC journal: <https://bcrec.id/>
E-mail: bcrec@live.undip.ac.id

On Wed, Oct 5, 2022 at 9:18 AM Puji Lukitowati Hariani <puji_lukitowati@mipa.unsri.ac.id> wrote:
Dear Prof. Dr. Istadi
Editor in Chief BCREC

I have read your request to proofread the manuscript, which has been accepted and is scheduled to publish shortly.
Along with this email, please find the attached files containing proofread manuscript (there is still one revision, highlighted), graphical abstract, and copyright transfer agreement.

I am looking forward to the publication of the manuscript. Thank you very much.

Sincerely yours

REVISION NOTE BASED ON REVIEWERS/EDITORS COMMENTS

Journal Name: Bulletin of Chemical Reaction Engineering & Catalysis

Manuscript ID: BCREC-2022-15788-53506-1-RV

Title of the manuscript: Synthesis of NiFe₂O₄/SiO₂/NiO Magnetic and Application for the Photocatalytic Degradation of Methyl Orange Dye under UV Irradiation

Author(s): Poedji Loekitowati Hariani, Muhammad Said, Addy Rachmat, Salni, Nabila Aprianti, Anisa Fitri Amatullah

Comment from Reviewer(s)	Answer/Revision Note	Location of Revision in Revised Manuscript
Reviewer 1: In the section on introduction, please add a space few words about the advanced oxidation processes for pollutants degradation based on the following works: https://doi.org/10.1016/j.cossms.2021.100941 https://doi.org/10.1007/s11356-018-3151-3	Thank you, and we have added about advanced oxidation processes for pollutant degradation following the literature suggestion	Introduction, reference [14] and [28], (blue-color highlighted)
Reviewer 1: The authors must explain photocatalysis's advantages over other methods in the light of the following works: https://doi.org/10.1016/j.jphotochem.2020.112665 https://doi.org/10.1016/j.jece.2021.106660	Thank you, and we have added photocatalysis's advantages over other methods following the literature suggestion	Introduction, reference [29], (blue-color highlighted)
Reviewer 1: The authors should investigate the effect of light source power.	I agree that light source power affects the effectiveness of photocatalytic degradation, but this study focuses on common aspects of photocatalytic degradation, pH, dose, initial concentration, and irradiation time. However, I have added in the discussion the importance of studying the influence of the power of the light source by citing as suggested.	Result and Discussion, Photocatalytic Degradation of Methyl Orange Dye. Reference [51] (blue-color highlighted)

Reviewer 1: Kindly add a photo for magnet separation of composite from treated solution with the prepared powder.	Thank you and we have added a photo for magnet separation from treated solution in Figure 5	Figure 5. Magnetic Properties of NiFe ₂ O ₄ , NiFe ₂ O ₄ /SiO ₂ , and NiFe ₂ O ₄ /SiO ₂ /NiO
Reviewer 1: For the photocatalytic degradation reaction of the dye (MO): How did you infer the holes and electrons drive the formation of •OH, h ⁺ , and O ₂ ^{•-} radicals? The authors should provide more approaches to prove this issue.	Thank you, and we have corrected the photocatalytic degradation reaction according to the reaction referring to the literature of Ammar et al. 2020 [53] and	Result and Discussion, Photocatalytic Degradation of Methyl Orange Dye. Reference [53] (blue-color highlighted)
Find the energy consumption of the photocatalytic system in optimal conditions. This was well presented and discussed in the following references https://doi.org/10.1002/clen.201000574 . It is suggested to cite which will be useful for authors and readers	Thank you, and we have added discussed in the following literature suggestion	Result and Discussion, Photocatalytic Degradation of Methyl Orange Dye. Reference [51] (blue-color highlighted)
Reviewer 1: The authors need to provide some structural characterization data after material degradation and demonstrate the stability of the material.	Thank you. The stability of the catalyst can be identified by the ability to be reused repeatedly. In this study, the catalyst used up to 5 cycles for the photocatalytic degradation process showed good performance. I have also added FTIR spectra of catalyst before and after photocatalytic degradation	Figure 10. FTIR spectra of NiFe ₂ O ₄ /SiO ₂ /NiO (a) before and (b) after reused five cycles for photocatalytic degradation (blue-color highlighted)
Reviewer 2: The blank experiment is very important. However, the authors only gave the degradation activity without irradiation. What is the degradation performance without NiFe ₂ O ₄ /SiO ₂ /NiO catalyst?	Thank you for the suggestion. Blank experiments have been carried out in this study but the percentage of degradation is very small at < 2% so in this study, it was ignored	-

<p>Reviewer 2: The authors said that NiFe₂O₄/SiO₂/NiO has the core, interlayer, and shell structure. But the core-interlayer-shell structure can't be seen from the SEM picture of NiFe₂O₄/SiO₂/NiO. It is suggested to add EDS-mapping characterization to observe the structure of the catalyst.</p>	<p>Thank you and we have added the EDS mapping in the manuscript</p>	<p>Figure 4. Elemental mapping of NiFe₂O₄/SiO₂/NiO (blue-color highlighted)</p>
--	--	--

Synthesis of NiFe₂O₄/SiO₂/NiO Magnetic and Application for the Photocatalytic Degradation of Methyl Orange Dye under UV Irradiation

Poedji Loekitowati Hariani^{1,*}, Muhammad Said¹, Addy Rachmat¹, Salni², Nabila Aprianti³, Anisa Fitri Amatullah¹

¹*Research Group on Magnetic Materials, Department of Chemistry, Faculty of Mathematics and Natural Sciences, Universitas Sriwijaya, Ogan Ilir 30662, Indonesia*

²*Department of Biology, Faculty of Mathematics and Natural Sciences, Universitas Sriwijaya, Ogan Ilir 30662, Indonesia*

³*Doctoral Program of Environmental Science, Graduate School, Universitas Sriwijaya, Palembang 30139, Indonesia*

* *Corresponding Author. E-mail: puji_lukitowati@mipa.unsri.ac.id*

Abstract

NiFe₂O₄/SiO₂/NiO magnetic was successfully synthesized using NiFe₂O₄, SiO₂, and NiO as the core, interlayer, and shell, respectively. NiFe₂O₄/SiO₂/NiO under UV light irradiation was used for photocatalytic degradation of methyl orange dye with different pH, catalyst dose, and initial dye concentration. This composite was characterized by X-ray Diffraction (XRD), Fourier Transform Infra-Red (FTIR), Scanning Electron Microscopy-Electron Dispersive X-ray Spectroscopy (SEM-EDs), Vibrating Sample Magnetometer (VSM), UV-Vis Diffuse Reflectance Spectroscopy (UV-Vis DRS), and Point of Zero Charge (pHpzc). The results showed that the composite is a superparamagnetic material with a saturation magnetization value of 44.13 emu/g. It also has a band gap of 2.67 eV with a pHpzc of 6.33. The optimum conditions for photocatalytic degradation were at pH of 4; 0.50 g/L catalyst dose, and 10 mg/L initial concentration. NiFe₂O₄/SiO₂/NiO degradation efficiency to methyl orange dye was 95.76%. The photocatalytic degradation in different concentrations follows the pseudo-first-order, where the greater the concentration, the smaller the constant rate (k). After five cycles of repeated use, NiFe₂O₄/SiO₂/NiO has good performance as a catalyst, efficient and favourable of a recyclable photocatalyst.

Keywords: NiFe₂O₄/SiO₂/NiO; magnetic; photocatalytic degradation; methyl orange dye

1. Introduction

Dye is an indispensable material in several industrial activities, such as textiles, food, cosmetics, pharmaceuticals, leather, paper, and soap [1,2]. Furthermore, synthetic dyes have a complex structure with toxic, carcinogenic, and mutagenic properties [3]. Dyes are easily soluble in water, difficult to degrade naturally, and has a long lifespan time in the environment. Dyes can also block the penetration of light into water, thereby inhibit the photosynthesis process and growth of aquatic organisms. The existence of dyes in the water interferes with aesthetics [4, 5]. Methyl orange is often used in industries and as a pH indicator in laboratories. It has a molecular formula, namely C₁₄H₁₄N₃SO₃Na, with a molecular weight of 327.34 g/mol. Furthermore, it is classified as anionic with an azo group (N=N). The aromatic amine group in its chemical structure is carcinogenic due to the production of benzidine compounds through biotransformation [6]. A previous study revealed that more than 50% of the dyestuffs used in industry are azo dyes [7].

Various methods have been used to reduce dyes including ultra-filtration [8], electrochemical degradation [9], coagulation-flocculation [10], precipitation [11], ion exchange removal [12], adsorption [5], and photocatalytic degradation [13]. Among these methods, the advanced oxidation processes based on reactive oxygen species (ROS) has attracted researchers in recent years [14]. This method has advantages such as the ability to convert pollutants from wastewater into less hazardous compounds, the process occurs in a short time and at room temperature. Moreover, it does not produce secondary toxic products, where organic pollutants can be mineralized into simpler and less toxic materials, such as mineral acids, CO₂, and H₂O [15].

Semiconductors can absorb photons equal to or more than the gap energy, causing the formation of positive holes and electrons. The positive hole reacts with water molecules and produce hydroxyl radicals (•OH). Electrons in the conduction band are trapped by oxygen to produce superoxide radicals (•O₂⁻). Furthermore, the interaction between hydroxyl, superoxide radicals, and dyes adsorbed on the semiconductor surface produces degradation products [16]. Several semiconductor materials can be

used for photocatalytic degradation of dyes, such as TiO_2 [17], NiO [18], ZnO [19], CuO [20], and BiVO_4 [21]. Nickel Oxide (NiO) is one of semiconductors, which is a p-type with a band gap range of 3.6–4.0 eV [22, 23]. It has high conductivity, stability, and catalytic properties. The material has also been used for the photodegradation of methylene blue, malachite green [24], orange II [18], and methyl orange [25].

The disadvantages of Nickel oxide as a catalyst include low adsorption capacity and a wide band gap. Semiconductors with wide band gap show low photon absorbing efficiencies, such as TiO_2 with 5% [26] and ZnO with 10% [27]. Other drawbacks are the recombination of photo-induced e^- , the separation of the catalyst after the photocatalytic degradation process, and the occurrence of corrosion in an acid or alkaline environment during the photocatalytic degradation process [28]. Therefore, is it necessary to increase catalyst and catalytic activity [29]. The modification of catalyst with other compounds can increase the effectiveness of degradation, for example incorporated catalys with magnetic compounds, separation can be easily and quickly using permanent magnets without filtering from aqueous media. The ferrite materials have the general formula MFe_2O_4 , where M is a divalent metal such as Ni, Fe, Cd, Mg, Cu, Co, and Zn [30]. One of these is NiFe_2O_4 , which has several advantages, including high electrical resistivity, chemical and mechanical stability, and excellent magnetic properties [31]. Modification of NiO with NiFe_2O_4 reduces the band gap of composite, where ferrite materials often have a band gap of ~ 2 [32].

To avoid the interaction between NiFe_2O_4 and NiO , another compound must be provided to serve as support [33]. SiO_2 can be used as a layer to prevent interaction. Another study reported that Fe_3O_4 coated with SiO_2 and TiO_2 as the outer thin layer could degrade methylene blue and ciprofloxacin dyes by 95% within 90 minutes [34]. SiO_2 can also protect ferrite compounds from agglomeration [35].

In this study, a core/interlayer/shell magnetic composite was synthesized, namely $\text{NiFe}_2\text{O}_4/\text{SiO}_2/\text{NiO}$. The product was characterized using XRD, FTIR, SEM-EDS, VSM, UV-Vis DRS, and pHpzc. $\text{NiFe}_2\text{O}_4/\text{SiO}_2/\text{NiO}$ was used for photocatalytic degradation of methyl orange dye under UV radiation. Therefore, this study aims to determine the effect of pH of a solution, initial dye concentration, and irradiation time on photocatalytic degradation ability, kinetics, and catalysts reusability.

2. Materials and Methods

2.1 Material

The chemicals used include $\text{Ni}(\text{NO}_3)_2 \cdot 6\text{H}_2\text{O}$, $\text{Fe}(\text{NO}_3)_3 \cdot 9\text{H}_2\text{O}$, NaOH , HCl , NH_4OH , methyl orange dye, tetraethyl orthosilicate (TEOS), ethanol from Merck, Germany, and distilled water.

2.2. Synthesis of NiFe_2O_4

The synthesis of NiFe_2O_4 was carried out using the coprecipitation method. A total of 6.58 g $\text{Ni}(\text{NO}_3)_2 \cdot 6\text{H}_2\text{O}$ and 15.62 g $\text{Fe}(\text{NO}_3)_3 \cdot 9\text{H}_2\text{O}$ were dissolved in 50 mL distilled water. The mixture was then stirred for 10 minutes and flowed with N_2 gas along with increasing temperature to 70°C . NaOH 2 M solution was gradually added to obtain a pH of ± 11 . The precipitate obtained, NiFe_2O_4 , was washed using distilled water and ethanol until neutral pH was achieved. The solid powder separated from the solution using an external magnet and dried in an oven at 80°C for 5 hours. Furthermore, it was calcined at 450°C for 2 hours.

2.3. Synthesis of $\text{NiFe}_2\text{O}_4/\text{SiO}_2$

$\text{NiFe}_2\text{O}_4/\text{SiO}_2$ was synthesized using a modified Stober method. A total of 4 g of NiFe_2O_4 was placed in a 250 mL Erlenmeyer, followed by adding 10 mL ethanol. The ultrasonic process is carried out for 2 hours. Subsequently, 10.8 mL of 25% ammonia solution was added, and the following ultrasonic process was continued for 1 hour. A total of 20 mL TEOS solution was then added gradually and ultrasonicated for ± 60 minutes. The precipitate ($\text{NiFe}_2\text{O}_4/\text{SiO}_2$) was separated using centrifugation at 8000 rpm for 20 minutes, and was washed with distilled water and ethanol until it reached a neutral pH. It was then separated from the solution using an external magnet and dried in the oven at 80°C for 5 hours, followed by calcination at 450°C for 2 hours.

2.4. Synthesis of $\text{NiFe}_2\text{O}_4/\text{SiO}_2/\text{NiO}$

The synthesis of $\text{NiFe}_2\text{O}_4/\text{SiO}_2/\text{NiO}$ was carried out based on the modified method by Wang *et al.* [36]. A total of 1 g of $\text{NiFe}_2\text{O}_4/\text{SiO}_2$, 110 mL of distilled water, and ethanol (1:1) were placed in a blue-cap glass bottle and sonicated for 80 minutes. After adding 4 g urea, the sonification process was continued for 30 minutes. Subsequently, 120 mL of 0.1 M $\text{Ni}(\text{NO}_3)_2 \cdot 6\text{H}_2\text{O}$ was added to the mixture, and sonification was carried out for 30 minutes. The precipitate ($\text{NiFe}_2\text{O}_4/\text{SiO}_2/\text{NiO}$), was separated from

the solution using an external magnet and dried in an oven at 105°C for 12 hours. The product was then washed with distilled water and separated using a centrifuge. It was dried in oven at 60°C for 6 hours and calcined at 400°C for 2 hours.

2.5. Characterization

NiFe₂O₄, NiFe₂O₄/SiO₂, and NiFe₂O₄/SiO₂/NiO were analyzed using X-ray Diffraction (XRD PANalytical X'Pert PRO), with Cu-K α radiation at $\lambda = 0.15418 \text{ \AA}$, 40 kV voltage, and range $2\theta = 10\text{-}90^\circ$. Furthermore, morphology and elemental composition were analyzed using Scanning electron microscopy equipped with an energy dispersive spectrometer (SEM-EDS JSM 6510). Fourier Transform Infrared (FTIR, Prestige 21, Shimadzu) used to determine the functional groups in the wave number 400-4000 cm⁻¹. Meanwhile, the Vibration Sample Magnetometer (VSM Oxford Type 1.2 T) helps to assess the magnetic hysteresis loop. The absorbance and band gap was determined using UV-Vis Diffuse Reflectance Spectroscopy (UV-Vis DRS) analysis (Orion Aquamate 8000) at a wavelength of 200-800 nm. The dye concentration was evaluated using a UV-Vis spectrophotometer (Type Orion Aquamate 8000). Total organic carbon was evaluated with the Total Organic Carbon Analyzer (TOC Teledyne Tekmar).

2.6. Point of Zero Charges (pHpzc) Determination

The determination of pHpzc was based on a modified procedure of Behzadi *et al.* [37], where 0.1 g of NiFe₂O₄/SiO₂/NiO was added to 25 mL of 0.1 M NaNO₃ solution. The pH value was adjusted to 2 -12 using 0.1 M HNO₃ solution and 0.1 M NaOH. The mixture was then stirred with a shaker for 2 hours and left for 24 hours. Initial and final pH was determined using a pH meter. Subsequently, pHpzc was evaluated from a graph plot of the initial pH of the solution Versus ΔpH .

2.7. Photocatalytic Activity

Photocatalytic degradation experiments were performed using the batch method with UV radiation of 40 W. The variables used include effect of pH (2-8), dose (0.25; 0.5; 0.75 and 1.0 g/L) and initial dye concentration (10, 20, 30 and 40 mg/L). The experiment was carried out in a closed reactor at room temperature. A total of 50 mL methyl orange dye was placed in the reactor and stirred for 40 minutes to obtain adsorption-desorption equilibrium, followed by irradiation for 20, 40, 60, 80, 100, 120,

and 140 minutes. The remaining dye after photocatalytic degradation was determined using a UV-Vis spectrophotometer. The ratio of the concentration for each time (C) with the initial concentration (C_0) was calculated using C/C_0 , while the degradation efficiency was expressed by the formula:

$$\text{Degradation efficiency} = \frac{C_0 - C}{C_0} \times 100\% \quad (1)$$

2.8. Reusability of NiFe₂O₄/SiO₂/NiO

NiFe₂O₄/SiO₂/NiO was applied for photocatalytic degradation of methyl orange dye under optimum conditions. Subsequently, it was washed with distilled water and dried in an oven for 3 hours at 70°C. Calcination was then carried out at 300°C for ± 2 hours to remove organic substances [38]. NiFe₂O₄/SiO₂/NiO was further reused for the process with a total of 5 repetitions.

3. Results and Discussion

3.1. Characterization of NiFe₂O₄, NiFe₂O₄/SiO₂, and NiFe₂O₄/SiO₂/NiO

The XRD spectra of NiFe₂O₄, NiFe₂O₄/SiO₂, and NiFe₂O₄/SiO₂/NiO are presented in Figure 1. NiFe₂O₄ XRD spectra showed a peak at $2\theta = 30.29^\circ$; 35.68° ; 43.39° ; 53.93° ; 57.45° ; 63.04° ; and 79.61° . The 2θ angle was in line with JCPDS No. 54-0964 (standard card NiFe₂O₄), namely 30.1° ; 35.3° ; 43.0° ; 53.7° ; 56.5° ; and 62.4° from the plane of 220, 311, 400, 422, 511, 440. Furthermore, the peak of NiFe₂O₄/SiO₂ appeared at the same angle, but decreased in intensity, namely 30.26° ; 35.67° ; 43.35° ; 53.89° ; 57.38° ; and 63.23° . Coating with SiO₂ showed a new peak with low intensity and wide at 2θ of 23° , which is a characteristic of its amorphous nature [39]. The XRD characterization of NiFe₂O₄/SiO₂/NiO showed the similar, namely 30.27° ; 35.72° ; 43.38° ; 53.85° ; 57.46° , and 63.21° . The addition of the peak was observed at an angle of 37.18° (111), and it also occurred in the spectra of NiO. Some of them also overlapped with those of NiFe₂O₄, such as 43.38° (200) and 63.21° (220). NiO also has the same peak, but it has a higher intensity than NiFe₂O₄ and NiFe₂O₄/SiO₂. The calculation results of the crystal size of NiFe₂O₄ using the Debye-Scherrer equation was 63.23 nm, while values of 53.56 nm and 48.53 nm were obtained for NiFe₂O₄/SiO₂ and NiFe₂O₄/SiO₂/NiO. The coating of NiFe₂O₄ with SiO₂ led to a decrease in crystal size because the material can prevent its agglomeration.

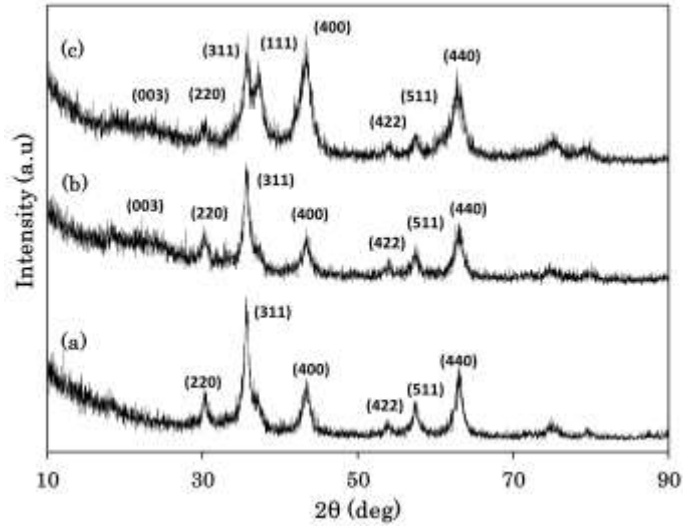


Figure 1. XRD pattern of (a) NiFe₂O₄, (b) NiFe₂O₄/SiO₂, and (c) NiFe₂O₄/SiO₂/NiO

The FTIR spectra of NiFe₂O₄, NiFe₂O₄/SiO₂, and NiFe₂O₄/SiO₂/NiO observed at wave numbers 400-4000 cm⁻¹ are presented in Figure 2. The results showed that all materials have broad peak at wavenumbers 3400 cm⁻¹ and 1600 cm⁻¹, indicating the presence of O-H groups from the water adsorbed by the catalyst [40]. The wave number of 400-700 cm⁻¹ are characteristics of stretching vibration metal-oxides, such as Fe-O and Ni-O. Fe-O stretching vibrations from NiFe₂O₄ appeared at all peaks, namely 580.57 cm⁻¹, 590.65 cm⁻¹, and 588.23 cm⁻¹. Strong peak asymmetry of Si-O-Si occurred at wave numbers of 1085.12 cm⁻¹ for NiFe₂O₄/SiO₂ and 1022.92 cm⁻¹ for NiFe₂O₄/SiO₂/NiO. In NiFe₂O₄/SiO₂/NiO, the Si-O-H vibrational bond was observed at 958.12 cm⁻¹ due to the interaction of SiO₂ with water molecules. This peak did not occur in NiFe₂O₄/SiO₂/NiO. Shi *et al.* [41] reported that a spinel structure of Ni²⁺-O bond was observed in the area around 470 cm⁻¹, in this study it was observed at 453.30 at 453.30 cm⁻¹ for NiFe₂O₄/SiO₂ and 459.69 cm⁻¹ for NiFe₂O₄/SiO₂/NiO.

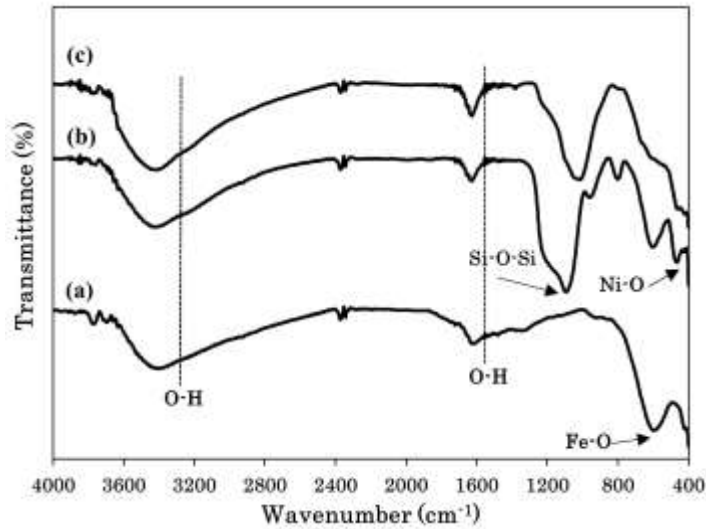
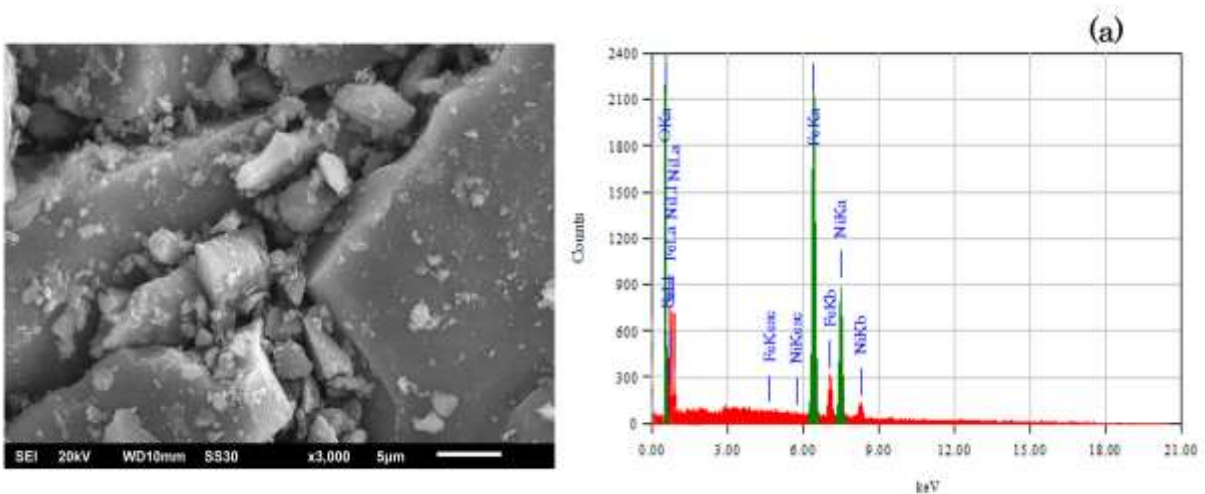


Figure 2. FTIR spectra of (a) NiFe_2O_4 , (b) $\text{NiFe}_2\text{O}_4/\text{SiO}_2$, and (c) $\text{NiFe}_2\text{O}_4/\text{SiO}_2/\text{NiO}$

The morphological differences between NiFe_2O_4 and $\text{NiFe}_2\text{O}_4/\text{SiO}_2$ are presented in Figure 3. NiFe_2O_4 was heterogeneous and large in size, while the surface of $\text{NiFe}_2\text{O}_4/\text{SiO}_2$ shows the presence of coating particles. $\text{NiFe}_2\text{O}_4/\text{SiO}_2/\text{NiO}$ morphology was more homogeneous with almost the same particle size. **Figure 4 shows the elemental mapping of $\text{NiFe}_2\text{O}_4/\text{SiO}_2/\text{NiO}$. Elements of Ni and O appear to spread on the catalyst's surface. This indicates that NiO has been distributed on the surface of $\text{NiFe}_2\text{O}_4/\text{SiO}_2$.** Table 1 shows the analysis results of the constituent elements of NiFe_2O_4 , $\text{NiFe}_2\text{O}_4/\text{SiO}_2$, and $\text{NiFe}_2\text{O}_4/\text{SiO}_2/\text{NiO}$ using EDS. NiFe_2O_4 is composed of elements, Ni, Fe, and O. The addition of Si indicates that SiO_2 has successfully coated NiFe_2O_4 . The increase in the percentage of Ni in $\text{NiFe}_2\text{O}_4/\text{SiO}_2/\text{NiO}$ shows indicates the addition of Ni from NiO.



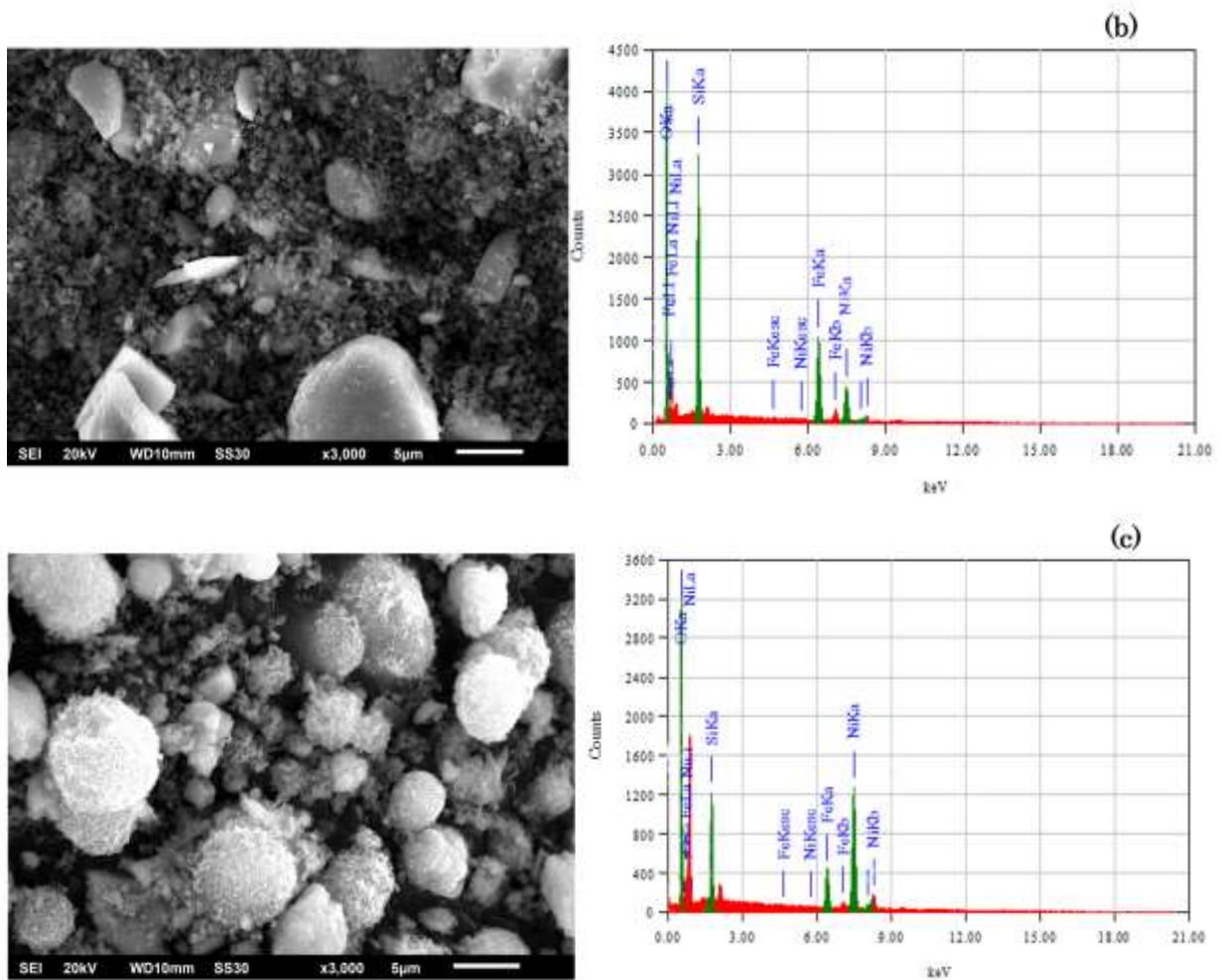


Figure 3. Morphology and EDS spectra of (a) NiFe_2O_4 , (b) $\text{NiFe}_2\text{O}_4/\text{SiO}_2$, and (c) $\text{NiFe}_2\text{O}_4/\text{SiO}_2/\text{NiO}$

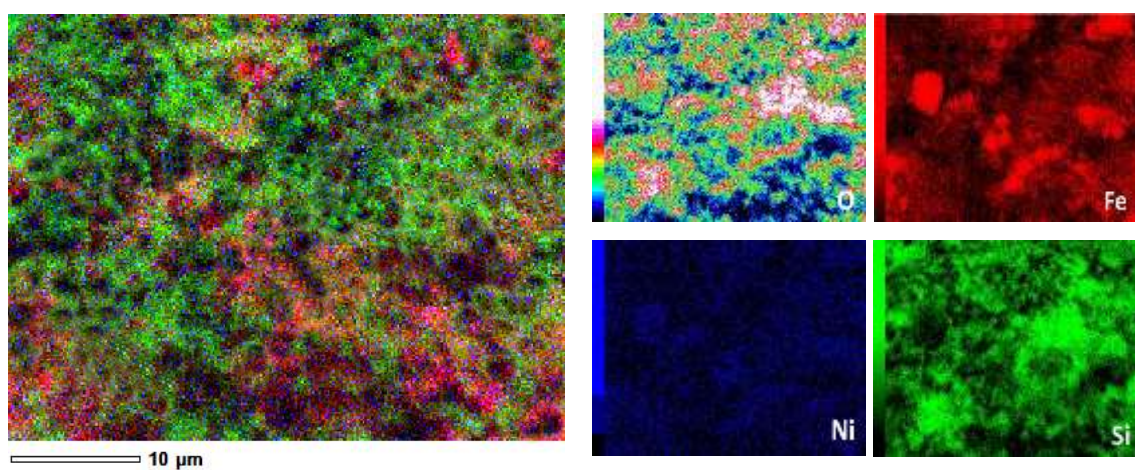
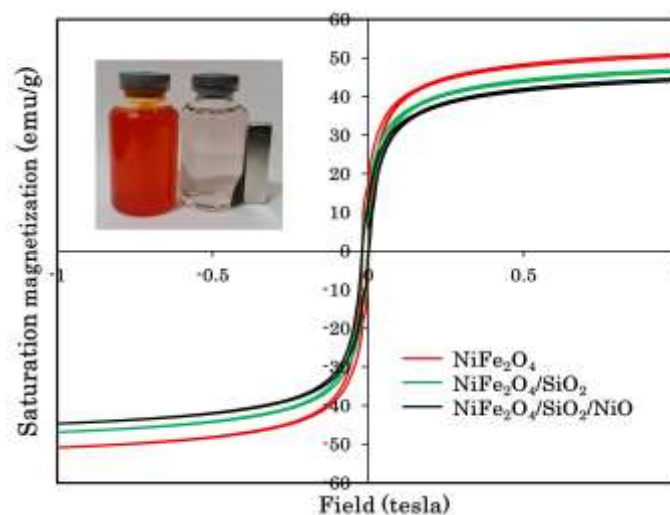


Figure 4. Elemental mapping of $\text{NiFe}_2\text{O}_4/\text{SiO}_2/\text{NiO}$

Table 1. Elemental composition of NiFe₂O₄, NiFe₂O₄/SiO₂, and NiFe₂O₄/SiO₂/NiO

Materials	Ni (%)	Fe(%)	O(%)	Si(%)
NiFe ₂ O ₄	24.99	46.63	27.36	-
NiFe ₂ O ₄ /SiO ₂	12.88	23.30	48.23	13.96
NiFe ₂ O ₄ /SiO ₂ /NiO	30.83	16.70	41.47	10.25

The magnetic properties of NiFe₂O₄, NiFe₂O₄/SiO₂, and NiFe₂O₄/SiO₂/NiO are presented in Figure 5. NiFe₂O₄ has a saturation magnetization value of 50.37 emu/g, which was greater than the value obtained after synthesis using solution combustion of 47.32 emu/g [42]. The bulk saturation value was 56 emu/g [43]. The saturation magnetization of NiFe₂O₄ was greater than NiFe₂O₄/SiO₂ and NiFe₂O₄/SiO₂/NiO by 46.37 emu/g and 44.13 emu/g, respectively. The magnetic properties decreased due to NiFe₂O₄ coating with non-magnetic SiO₂, which isolated NiFe₂O₄ from the magnetic field. Another study reported that the saturation magnetization value decreased as follows: CoFe₂O₄ > CoFe₂O₄/SiO₂ > CoFe₂O₄/SiO₂/TiO₂ [44]. Magnetic properties are influenced by crystal size. The larger the crystal size, the greater the saturation magnetization [45]. In this study, the largest crystal size was obtained from NiFe₂O₄.

**Figure 5.** Magnetic properties of NiFe₂O₄, NiFe₂O₄/SiO₂, and NiFe₂O₄/SiO₂/NiO

The amount of energy absorbed by the catalyst depends on the optical band gap energy, namely the difference between the valence and conduction bands. The decrease in the gap (E_g) by the doping process prevents electron-hole pair recombination (e^-/h^+) and increases photocatalytic activity [46]. The optical E_g was determined using the following equation [41]:

$$\alpha h\nu = A(h\nu - E_g)^n \quad (2)$$

Where α is the absorption coefficient, h is Planck's constant, and n is the light frequency. The value of n was $\frac{1}{2}$ for direct semiconductors, while a value of 2 was obtained for indirect variants. NiO is a catalyst that is classified as a direct semiconductor. A in the formula is the proportionality constant, and E_g is the optical band gap.

The analysis of optical properties using UV-Vis DRS is shown in Figure 6. The wavelength obtained in this study from 200-800 nm. Band gap value is obtained from the curve of $(\alpha h\nu)^2$ Versus $h\nu$ (photon energy). The NiFe₂O₄ band gap was 1.81 eV, which was lower than NiFe₂O₄/SiO₂ and NiFe₂O₄/SiO₂/NiO by 2.21 eV and 2.67 eV, respectively. Another study reported that semiconductor doping using ferrite compounds reduced the band gap. For example, the band gap for ZnO decreased by 3.12 eV to 1.71 eV after doping by NiFe₂O₄ [46].

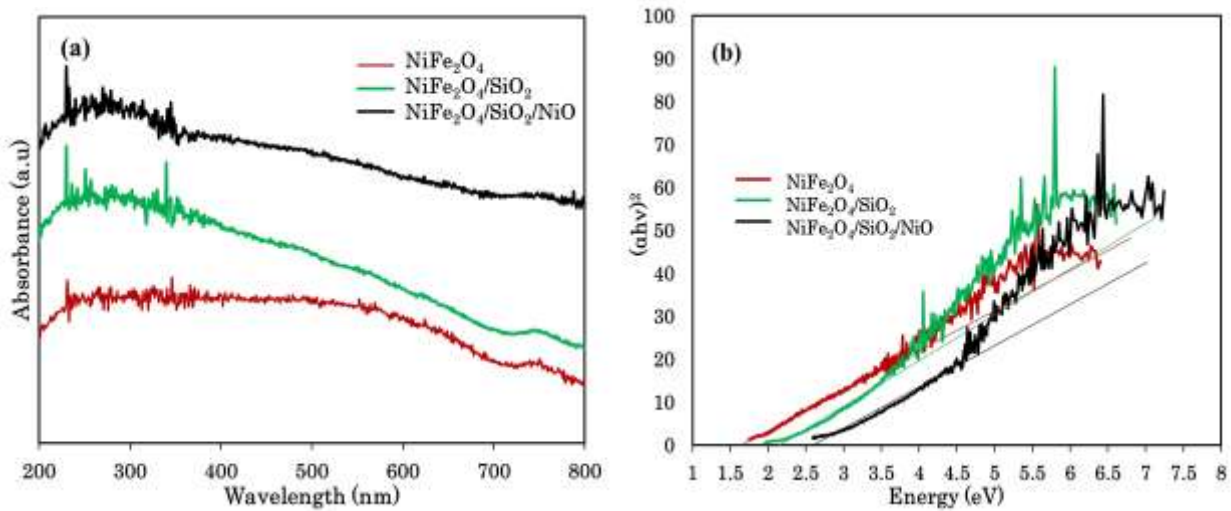


Figure 6. Spectra of (a) UV-Vis DRS and (b) Band gap energies of NiFe₂O₄, NiFe₂O₄/SiO₂, and NiFe₂O₄/SiO₂/NiO

3.2. Photocatalytic Degradation of Methyl Orange Dye

Photocatalytic degradation using NiFe₂O₄/SiO₂/NiO on methyl orange dye carried out through the batch method by analyzing the effect of pH, catalyst dose, and dye concentration on dye removal with an irradiation time of 0-140 minutes (interval 20 minutes). Figure 7a shows a graph of the initial pH Versus Δ pH plot to obtain pH_{zpc} with a value of 6.33. The material surface has a negative and positive charge when pH_{zpc} < pH and pH_{zpc} > pH, respectively [47]. Figure 7b shows the effect of pH on the amount of degraded methyl orange dye, which had a 50 mL volume and 20 mg/L

concentration of methyl orange dye. The methyl orange dye had a pH in a range of 3.1-4.5 [48]. At $\text{pH} < \text{pH}_{\text{pzc}}$, $\text{NiFe}_2\text{O}_4/\text{SiO}_2/\text{NiO}$ is positively charged, while methyl orange dye is anionic (negatively charged), causing an attraction between them.

A control was carried out without irradiation for 40 minutes to create adsorption-desorption equilibrium, and the C/C_0 curve shows a sloping trend. Meanwhile, it decreased sharply with irradiation, indicating rapid degradation. The same phenomenon occurred in the photocatalytic degradation of rhodamine B dye using $\gamma\text{-Fe}_2\text{O}_3@\text{SiO}_2@\text{TiO}_2$. The addition of catalyst for one hour without irradiation showed that the degradation percentage was less than 10% [49]. In this study, the highest degradation efficiency was at pH of 4. The higher the pH, the more the hydroxide ions (OH^-), which causes competition between the dye and hydroxide ions. Another study reported that the highest degradation efficiency for methyl orange dye occurred at a pH of 4 using $\text{CoFe}_2\text{O}_4/\text{SiO}_2/\text{TiO}_2$ [35].

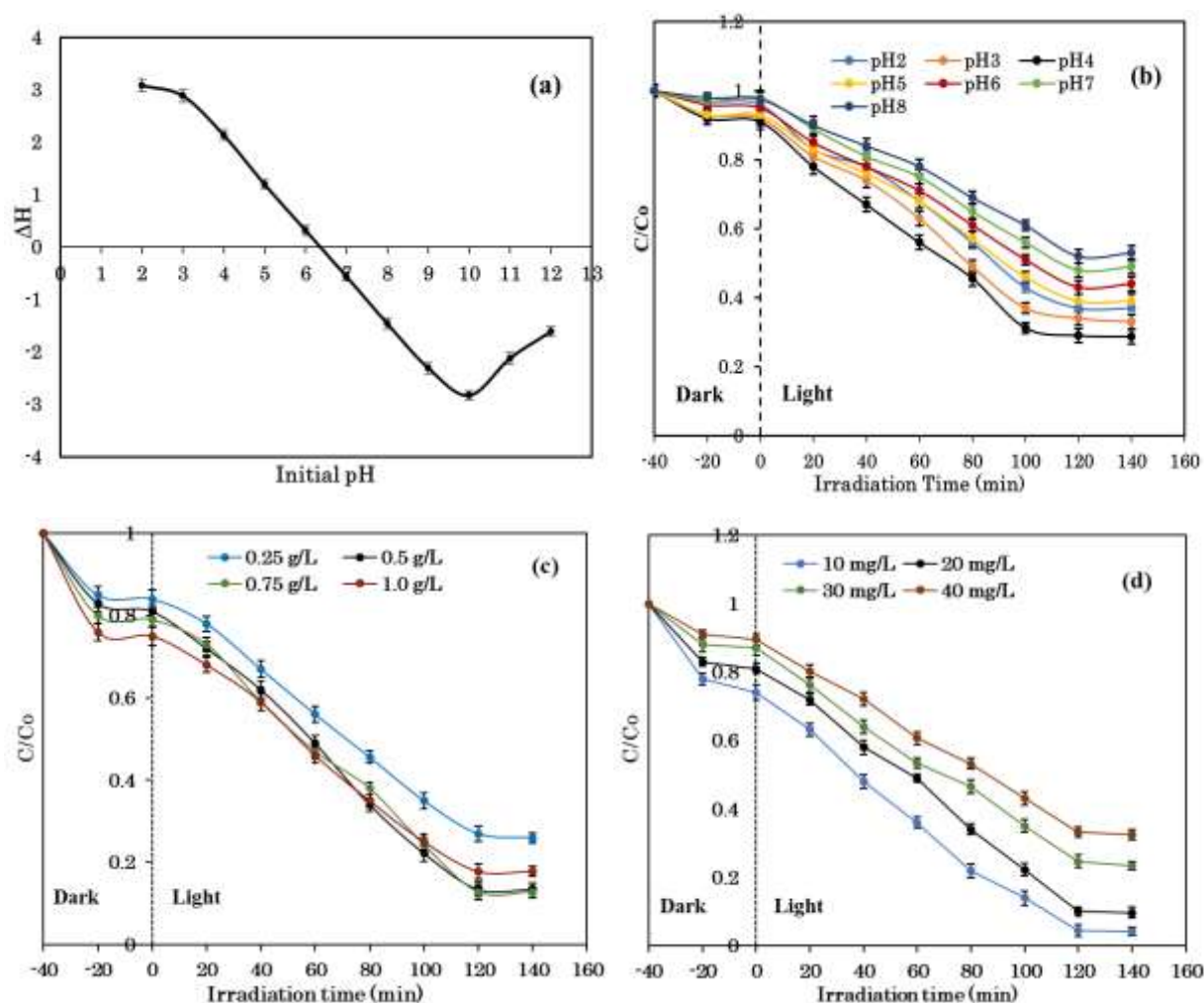


Figure 7. (a) pH_{pzc} $\text{NiFe}_2\text{O}_4/\text{SiO}_2/\text{NiO}$, and photocatalytic degradation curve of methyl orange dye as a function of (b) pH, (c) Initial concentration, and (d) $\text{NiFe}_2\text{O}_4/\text{SiO}_2/\text{NiO}$ doses

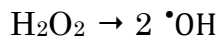
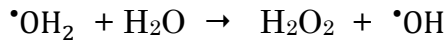
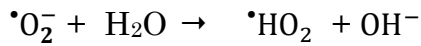
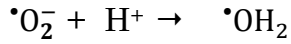
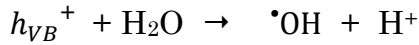
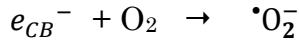
The effect of catalyst dose on the photocatalytic degradation of methyl orange was analyzed using different catalyst concentrations from 0.25 to 1.0 g/L. The results obtained are presented in Figure 7c. At 0-40 minutes, the percentage of dye degradation increased drastically from a dose of 0.25 to 1.0 g/L. However, there was no increase after 120 minutes. The higher the catalyst dose, the more active sites (hydroxyl free radicals) are available, which leads to more degradation. The solution becomes cloudy and opaque when excess catalyst is added, reducing light transmission to the dye [48]. Alkaykh *et al.* [50] reported that at high doses of catalyst, molecular activation was inhibited due to collisions between catalysts, which reduced the reaction rate. The optimum dose obtained was 0.5 g/L with a degradation efficiency of 86.56%.

Figure 7d shows that the greater the concentration of the dye, the smaller the degraded substance. Furthermore, the higher the concentration, the more it can interact with the active surface of the catalyst, but this condition prevents the penetration of light [35]. The smallest value of C/C_0 was obtained from 10 mg/L of methyl orange with degradation efficiency of 95.76%. **In this study, UV light was used as an irradiation source with a constant intensity. The effectiveness of photocatalytic degradation can be increased by optimizing the use of energy consumption, which is the most suitable intensity for the photocatalytic degradation process [51].** Table 2 shows the comparison of several photocatalyst for the methyl orange dye degradation, where NiFe₂O₄/SiO₂/NiO had a better degradation efficiency than others.

Table 2. Comparison of several photocatalysts for the methyl orange dye degradation

Catalyst	pH	Dosis (g/L)	Concentration (mg/L)	Time (min)	Efficiency (%)	Reff.
NiO	2	2.0	10	30	90	24
Fe ₃ O ₄ /SiO ₂ /TiO ₂	-	0.25	30	300	90.2	39
MnO ₂ /CeO ₂	2.6	1.0	10	60	90	52
Chitosan-Zn-Mg	3	0.15	10	120	74.05	4
TiO ₂	3	-	15	240	93	53
NiFe ₂ O ₄ /SiO ₂ /NiO	4	0.50	10	120	95.76	In this work

The photocatalytic degradation mechanism of the dye methyl orange dye (MO) is described as follows [54]:



The first reaction is the adsorption of MO on the surface of the catalyst. Conduction band electrons (e_{CB}^-) and valence band holes (h_{VB}^+) are photogenerated when $\text{NiFe}_2\text{O}_4/\text{SiO}_2/\text{NiO}$ is exposed to UV irradiation which is greater than the band gap energy. The adsorbed hydroxyl ions and oxygen on the catalyst with the MO form hydrogen bonds. MO on the catalyst surface will be attacked by $\cdot\text{OH}$ and $\cdot\text{O}_2^-$, resulting in decolorization [46,54].

Total organic carbon analysis can determine the mineralization level of dyes obtained from photocatalytic degradation. The level was not fully achieved, but it indicates the occurrence of the mineralization process [55]. For example, the TOC removal for phenol using $\text{CoFe}_2\text{O}_4/\text{SiO}_2/\text{TiO}_2$ in 120 minutes was 87%, and the TOC removal of paraquat after 180 minutes using N-doped $\text{TiO}_2@\text{SiO}_2@\text{Fe}_3\text{O}_4$ was 84.71% [35,55]. In this study, the initial and after-degradation TOC values were determined under optimum conditions: pH of 4, 0.5 g/L photocatalyst dose, methyl orange dye concentration of 10 mg/L, and irradiation time of 120 minutes. The TOC removal value obtained was 87.60%. These results indicated that the dye had been decomposed into minerals, such as H_2O and CO_2 , and the remnants have been converted into other organic materials.

3.3. Photocatalytic Degradation Kinetics

Photocatalytic degradation can be illustrated using pseudo-first-order [56], and the equation is as follows:

$$\ln C_0/C_t = k t \quad (3)$$

Where C_0 and C_t are the initial concentration and concentration of dye at the time (mg/L), k is the rate constant (min^{-1}), and t is the irradiation time (min). The initial concentration of the dye has a fundamental effect on the degradation rate, where the kinetic rate constant decreases as the concentration increases [57]. Figure 8 shows a pseudo-first-order graph with varying methyl orange dye levels of 10, 20, 30, and 40 mg/L. The correlation coefficient (R^2) value indicates the suitability of photocatalytic degradation, which was close to 1. Furthermore, the k values obtained were 0.0212, 0.0157, 0.0112 and 0.0083 min^{-1} . Li *et al.*, [56] reported that the degradation rate of semiconductors was predicted to follow the Langmuir–Hinshelwood type of kinetics and first-order decomposition, assuming the degradation occurs directly on the surface of the catalyst. Another study reported that the kinetics constants obtained for methyl orange dye using TiO_2 decreased as the concentration increased (0.015, 0.025, and 0.035 g/L), namely $0.00278 > 0.0023 > 0.00173 \text{ min}^{-1}$ [53].

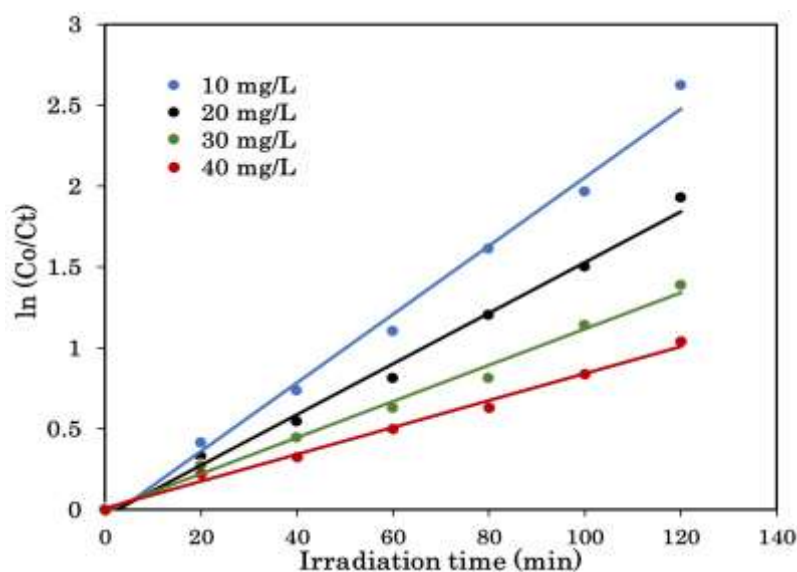


Figure 8. The photocatalytic degradation kinetics of $\text{NiFe}_2\text{O}_4/\text{SiO}_2/\text{NiO}$ in different methyl orange dye concentration

3.4. Photocatalyst Reusability

Evaluation of the stability and ability of $\text{NiFe}_2\text{O}_4/\text{SiO}_2/\text{NiO}$ used is presented in Figure 9. After its usage in the photocatalytic degradation process, it was separated from the solution using a permanent magnet. This catalyst was cleaned with deionization water and then calcined. Subsequently, it was reused for photocatalytic degradation of methyl orange dye. Five cycles showed a change in its ability from

98.51 to 95.36%. These results showed the adequate performance of $\text{NiFe}_2\text{O}_4/\text{SiO}_2/\text{NiO}$ as a photocatalyst.

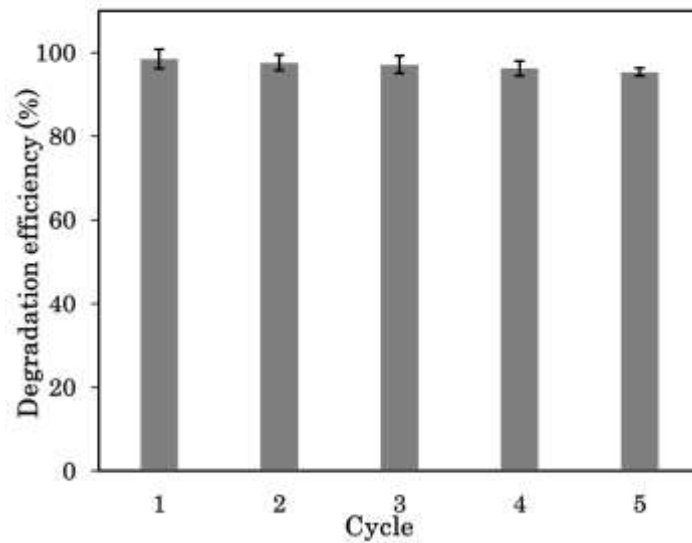


Figure 9. Reusability of $\text{NiFe}_2\text{O}_4/\text{SiO}_2/\text{NiO}$ for photocatalytic degradation of methyl orange dye

The FTIR spectra of $\text{NiFe}_2\text{O}_4/\text{SiO}_2/\text{NiO}$ before and after being used as a catalyst showed similar spectra as shown in Figure 10. This indicates that the catalyst has high stability under UV light irradiation. The functional groups of the catalyst before and after use were the same, although there was a slight change in intensity.

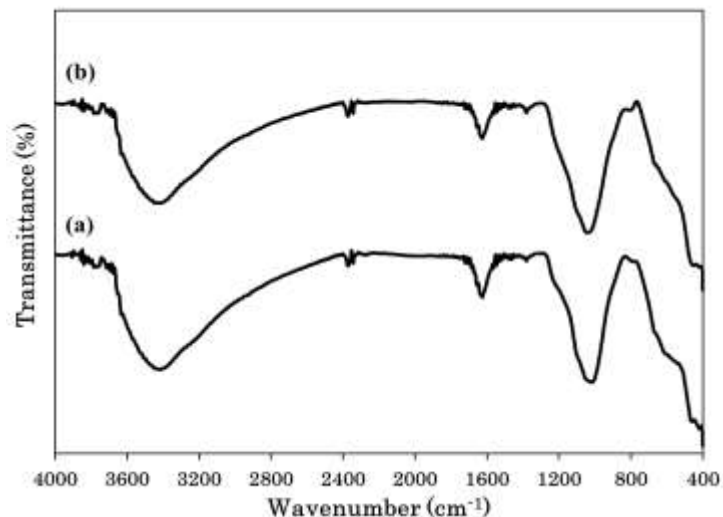


Figure 10. FTIR spectra of $\text{NiFe}_2\text{O}_4/\text{SiO}_2/\text{NiO}$ (a) before and (b) after reused five cycles for photocatalytic degradation

4. Conclusions

In this study, a core/interlayer/shell magnetic composite was successfully synthesized, namely $\text{NiFe}_2\text{O}_4/\text{SiO}_2/\text{NiO}$, with a saturation magnetization value of

44.13 emu/g and a band gap of 2.67 eV. The EDS results confirmed that the product consisted of Ni, Fe, O, and Si, which indicated that the synthesis was successful. Photocatalytic degradation of methyl orange dye by NiFe₂O₄/SiO₂/NiO under UV irradiation at pH 4, 0.5 g/L dose of catalyst, and 10 mg/L concentration of methyl orange dye for 120 minutes irradiation, has a degradation efficiency of 95.76%. The indicated that the mineralization of methyl orange dye by the effectiveness of the TOC was 87.60%. Experimental data showed that the photocatalytic degradation kinetics according a pseudo-first-order. NiFe₂O₄/SiO₂/NiO has high stability and catalytic activity it was used in five cycles. Along with its low cost, high photocatalytic activity, stability, and easy separation by external magnet, the NiFe₂O₄/SiO₂/NiO has broad prospects in large-scale wastewater treatment.

Acknowledgment

Author would thank to the Ministry of Education, Culture, Research and Technology for funded research of Penelitian Dasar Unggulan Perguruan Tinggi (PDUPT) scheme in 2022, under the contract No. 0063.01/UN9.3.1/PL/2022.

References

- [1] Gusmao, K.A.G., Gurgel, L.V.A., Melo, T.M.S., Gil, L.F. (2013). Adsorption Studies of Methylene Blue and Gentian Violet on Sugarcane Bagasse Modified with EDTA Dianhydride (EDTAD) in Aqueous Solutions: Kinetic and Equilibrium Aspects. *Journal of Environmental Management*, 118, 135-143. DOI: 10.1016/j.jenvman.2013.01.017
- [2] Ali, N., Said, A., Ali, F., Razig, F., Ali, Z., Bilal, M., Reinert, L., Iqbal, H.M.N. (2020). Photocatalytic Degradation of Congo Red Dye from Aqueous Environment Using Cobalt Ferrite Nanostructures: Development, Characterization, and Photocatalytic Performance. *Water, Air, & Soil Pollution*, 231(50), 1-16. DOI: 10.1007/s11270-020-4410-8
- [3] Iwuozor, K., Ighalo, J.O, Emenike, E.C., Ogunfowora, L.A., Igwegbe, C.A. (2021). Adsorption of Methyl Orange: A Review on Adsorbent Performance. *Current Research in Green and Sustainable Chemistry*, 4, 1-6. DOI: 10.1016/j.crgsc.2021.100179
- [4] Makeswari, M., Saraswathi, P. (2020). Photocatalytic Degradation of Methylene Blue and Methyl Orange from Aqueous Solution using Solar Light

- onto Chitosan Bi-metal Oxide Composite. *SN Applied Science*, 2(336), 1-12. DOI:10.1007/s42452-020-1980-4
- [5] Alghamdi, A.A., Al-Odayni, A., Saeed, W.S., Almutairi, M.S., Alharthi, F.A., Aouak, T., Al-Kahtani, A. (2019). Adsorption of Azo Dye Methyl Orange from Aqueous Solutions Using Alkali-Activated Polypyrrole-Based Graphene Oxide. *Molecules*, 24, 1-17. DOI: 10.3390/molecules24203685
- [6] Chen, D., Chen, J., Luan, X., Ji, H., Xia, Z. (2011). Characterization of Anion-Cationic Surfactants Modified Montmorillonite and Its Application for the Removal of Methyl Orange. *Chemical Engineering Journal*, 171, 1150-1158. DOI: 10.1016/j.cej.2011.05.013
- [7] Ajmal, A., Majeed, I., Malik, R.N., Idriss H., Nadeem, M.A. (2014). Principles and Mechanisms of Photocatalytic Dye Degradation on TiO₂ Based Photocatalysts: a Comparative Overview. *RSC Advances*, 4, 37003-37026. DOI: 10.1039/C4RA06658H
- [8] Fradj, A.B., Boubakri, A., Hafiane, A., Hamouda, S.B. (2020). Removal of Azoic Dyes from Aqueous Solutions by Chitosan Enhanced Ultrafiltration. *Results in Chemistry*, 2, 1-9. DOI: 10.1016/j.rechem.2019.100017
- [9] Li, S., Zhao, Y., Chu, J., Li, W., Yu, H., Liu, G. (2013). Electrochemical Degradation of Methyl Orange on Pt-Bi/C Nanostructured Electrode by a Square-wave Potential Method. *Electrochimica Acta*, 92, 93-101. DOI: 10.1016/j.electacta.2013.01.012
- [10] Igwegbe, C.A., Onukkwuli, O.D., Ighalo, J.O., Umembamalu, C.J. (2021), Electrocoagulation-flocculation of Aquaculture Effluent using Hybrid Iron and Aluminium Electrodes: A comparative Study. *Chemical Engineering Journal Advances*, 6,1-14. DOI: 10.1016/j.cej.2021.100107
- [11] Ali, M., Sarkar, A., Pandey, M.D., Pandey, S. (2006). Efficient Precipitation of Dyes from Dilute Aqueous Solutions of Ionic Liquids. *Analytical Sciences*, 22, 1051-1053. DOI: 10.2116/analsci.22.1051
- [12] Huang, R., Zhang, Q., Yao, H., Lu, Z., Zhou, Q., Yan, D. (2021). Ion-Exchange Resins for Efficient Removal of Colorants in Bis(hydroxyethyl) Terephthalate. *ACS Omega*, 6(18), 12351-12360. DOI: 10.1021/acsomega.1c01477
- [13] Hanif, M.K.H.M., Sapawe, N. (2020). A Short Review on Photocatalytic toward Dye Degradation. *Materials Today*, 31(1), A42-A47. DOI: 10.1016/j.matpr.2020.10.967

- [14] Hassani, A., Krishnan, S., Scaria J., Eghbali, P., Nidheesh, P.V. (2021). Z-scheme Photocatalysts for Visible-light-driven Pollutants Degradation: A Review on Recent Advancements. *Current Opinion in Solid State and Materials Science*, 25(5), 1-25. DOI: 10.1016/j.cossms.2021.100941
- [15] Solomon, R.V., Lydia, I.S., Merlin, J.P., Venuvanalingam, P. (2012). Enhanced Photocatalytic Degradation of Azo Dyes using Nano Fe₃O₄. *Journal of the Iranian Chemical Society*, 9, 101-109. DOI: 10.1007/s13738-011-0033-8
- [16] Kitture, R., Koppikar, S.J., Kaul-Ghanekar, R., Kale, S.N. (2011). Catalyst Efficiency, Photostability and Reusability Study of ZnO Nanoparticles in Visible Light for Dye Degradation. *Journal of Physics and Chemistry of Solids*, 27(1), 60-66. DOI: 10.1016/j.jpccs.2010.10.090
- [17] Lee, S.Y., Kang, D., Jeong, S., Do, H. T., Kim, J. H. (2020). Photocatalytic Degradation of Rhodamine B Dye by TiO₂ and Gold Nanoparticles Supported on a Floating Porous Polydimethylsiloxane Sponge under Ultraviolet and Visible Light Irradiation. *ACS Omega*, 5(8), 4233-4241. 10.1021/acsomega.9b04127
- [18] Khan, N.A., Saeed, K., Khan, I., Gul, T., Sadiq, M., Uddin, A., Zakker I. (2022). Efficient Photodegradation of Orange II Dye by Nickel Oxide Nanoparticles and Nanoclay Supported Nickel Oxide Nanocomposite. *Applied Water Science*, 12(131), 1-10. DOI: 10.1007/s13201-022-01647-x
- [19] Isai, K.A., Shrivastava, V.S. (2019). Photocatalytic Degradation of Methylene Blue using ZnO and 2%Fe–ZnO Semiconductor Nanomaterials Synthesized by Sol–Gel Method: a Comparative Study. *SN Applied Sciences*, 1(1247), 1-11. DOI: 10.1007/s42452-019-1279-5
- [20] Nazim, M., Khan, A.A.P., Asiri, A.M., Kim, J.H. (2021). Exploring Rapid Photocatalytic Degradation of Organic Pollutants with Porous CuO Nanosheets: Synthesis, Dye Removal, and Kinetic Studies at Room Temperature. *ACS Omega*, 6, 2601-2612. DOI: 10.1021/acsomega.0c04747
- [21] Hunge, Y.M., Uchida, A., Tominaga, Y., Fujii, Y., Ydav, A.A., Kang, S., Suzuki, N., Shitanda, I., Kondo, T., Itagaki, M., Yuasa, M., Gosavi, S., Fujishima, A., Terashima, C. (2021). Visible Light-Assisted Photocatalysis Using Spherical-Shaped BiVO₄ Photocatalyst. *Catalysts*, 11(4), 1-11. DOI: 10.3390/catal11040460
- [22] Bordbar, M., Negahdar, N., Nasrollahzadeh, M. (2018). *Melissa Officinalis* L. Leaf Extract Assisted Green Synthesis of CuO/ZnO Nanocomposite for the

- Reduction of 4-nitrophenol and Rhodamine B. *Separation and Purification Technology*, 191, 295-300. DOI: 10.1016/j.jphotobiol.2018.03.016.
- [23] Kganyago, P., Mahlaule-Glory, L.M., Mathipa, M.M., Ntsendwana, B., Mketso, N., Mbita, Z., Hintsho-Mbita N.C. (2018). Synthesis of NiO Nanoparticles via a Green Route using *Monsonia burkeana*: The Physical and Biological Properties. *Journal of Photochemistry and Photobiology B: Biology*, 182, 18-26. DOI: 10.1016/j.jphotobiol.2018.03.016
- [24] Motene, K., Mahlaule-Glory, L.M., Ngoepe, N.M., Mathipa, M.M., HintshoMbita, N.C. (2021). Photocatalytic Degradation of Dyes and Removal of Bacteria using Biosynthesised Flowerlike NiO Nanoparticles. *International Journal of Environmental Analytical Chemistry*, 2021, 1-17. DOI: 10.1080/03067319.2020.1869730
- [25] Barzinjy, A.A., Hamad, S.M. Aydin, S., Ahmed, M.H., Hussain, F.H.S. (2020). Green and Eco-friendly Synthesis of Nickel Oxide Nanoparticles and Its Photocatalytic Activity for Methyl Orange Degradation. *Journal of Materials Science: Materials in Electronics*, 31, 11303–11316. DOI: 10.1007/s10854-020-03679-y
- [26] Moosavi, S., Li, R.Y.M., Lai, C.W., Yusof, Y., Gan, S., Akbarzadeh, O., Chowhurry, Z.Z., Yue, X., Johan, M.R. (2020). Methylene Blue Dye Photocatalytic Degradation over Synthesised Fe₃O₄/AC/TiO₂ Nano-Catalyst: Degradation and Reusability Studies. *Nanomaterials*, 10(12), 1-15. DOI: 10.3390/nano10122360
- [27] Rahimi, S.M., Panahi, A.H., Moghadam, N. S. M., Allahyari, E., Nasseh, N. (2022). Breaking Down of Low-biodegradation Acid Red 206 Dye using Bentonite/Fe₃O₄/ZnO Magnetic Nanocomposite as a Novel Photo-catalyst in Presence of UV light. *Chemical Physics Letters*, 794, 1-11. DOI: 10.1016/j.cplett.2022.139480
- [28] Hassani, A., Faraji, M., Eghbali, P. (2020). Facile Fabrication of mpg-C₃N₄/Ag/ZnO Nanowires/Zn Photocatalyst Plates for Photodegradation of Dye Pollutant. *Journal of Photochemistry and Photobiology A: Chemistry*, 400, 1-15. DOI: 10.1016/j.jphotochem.2020.112665
- [29] Madihi-Bidgoli, S., Asanezhad, S., Yaghoot-Nezhad, A., Hassani, A. (2021). Azurobine Degradation using Fe₂O₃@multi-walled Carbon Nanotube Activated Peroxymonosulfate (PMS) under UVA-LED Irradiation: Performance,

- [30] Hirthna, Sendhilnathan, S., Rajan, P.I., Adinaveen, T. (2018). Synthesis and Characterization of NiFe₂O₄ Nanoparticles for the Enhancement of Direct Sunlight Photocatalytic Degradation of Methyl Orange. *Journal of Superconductivity and Novel Magnetism*, 31, 1-9. DOI: 10.1007/s10948-018-4601-3
- [31] Ishino, K., Narumiya, Y. (1988). Development of Magnetic Ferrites: Control and Application of Loss. *Ceramic Bulletin*, 66, 1469-1475. DOI:10.1002/CHIN.198820306
- [32] Casbeer, E., Sharma, V.K., Li, X.Z. (2012). Synthesis and Photocatalytic Activity of Ferrites under Visible Light: A Review. *Separation and Purification Technology*, 87, 1-14. DOI: 10.1016/j.seppur.2011.11.034.
- [33] Shan, A. Y., Ghazi, T. I. M., Rashid, S. A. (2010). Immobilisation of Titanium Dioxide onto Supporting Materials in Heterogeneous Photocatalysis: a Review. *Applied Catalysis A: General*, 389 (1), 1-8. DOI: 10.1016/j.apcata.2010.08.053
- [34] Teixeira, S., Mora, H., Blasse L., Martins, P.M., Carabineiro, S.A.C., Lanceros-Mendez, S., Kuhn, K., Cuniberti, G. (2017). Photocatalytic Degradation of Recalcitrant Micropollutants by Reusable Fe₃O₄/SiO₂/TiO₂ Particles. *Journal of Photochemistry and Photobiology A: Chemistry*, 345, 27-35. DOI: 10.1016/j.jphotochem.2017.05.024
- [35] Hariani P.L., Said M., Salni, Aprianti N. and Naibaho Y.A.L.R. (2022). High Efficient Photocatalytic Degradation of Methyl Orange Dye in an Aqueous Solution by CoFe₂O₄-SiO₂-TiO₂ Magnetic Catalyst. *Journal of Ecological Engineering*, 23, 118-128. DOI: 10.12911/22998993/143908
- [36] Wang, L., Huang, Y., Sun, X., Huang, H., Liu, P., Zong, M., Wang, Y. (2014). Synthesis and Microwave Absorption Enhancement of Graphene@Fe₃O₄@SiO₂@NiO Nanosheet Hierarchical Structures. *Nanoscale*, 6, 3157-3164. DOI: 10.1039/C3NR05313J
- [37] Behzadi, S, Nonahal, B., Royaeae, S.J., Asadi, A.A. (2020). TiO₂/SiO₂/Fe₃O₄ Magnetic Nanoparticles Synthesis and Application in Methyl Orange UV Photocatalytic Removal. *Water Science Technology*, 82 (11), 2432-2445. DOI: 10.2166/wst.2020.509

- [38] Prasad, K.S., Shamshuddin, S.Z.M. (2022). Highly Efficient Conversion of Glycerol and t-Butanol to Biofuel Additives over AlPO Solid Acid Catalyst under Microwave Irradiation Technique: Kinetic Study. *Comptes Rendus Chimie*, 25, 149-170. DOI: 10.5802/crchim.132
- [39] Chen, F., Yan, F., Chen, Q., Wang, Y., Han, L. (2014). Fabrication of Fe₃O₄@SiO₂@TiO₂ Nanoparticles Supported by Graphene Oxide Sheets for the Repeated Adsorption and Photocatalytic Degradation of Rhodamine B under UV Irradiation. *Dalton Transaction*, 43, 13537-13544. DOI: 10.1039/C4DT01702A
- [40] Alzahrani, E. (2017). Photodegradation of Binary Azo Dyes Using Core-Shell Fe₃O₄/SiO₂/TiO₂ Nanospheres. *American Journal of Analytical Chemistry*, 8, 95-115. DOI: 10.4236/ajac.2017.81008
- [41] Shi, M., Qiu, T., Tang, B., Zhang, G., Yao, R., Xu, W., Chen, J., Fu, X., Ning, H., Peng, J. (2021). Temperature-Controlled Crystal Size of Wide Band Gap Nickel Oxide and Its Application in Electrochromism. *Micromachines*, 12(80), 1-11. DOI: 10.3390/mi12010080.
- [42] Hariani P.L., Said M., Rachmat A., Riyanti F., Pratiwi H.C. Rizki W.T. (2021), Preparation of NiFe₂O₄ Nanoparticles by Solution Combustion Method as Photocatalyst of Congo red. *Bulletin of Chemical Reaction Engineering & Catalysis*, 16, 481-490. DOI: 10.9767/bcrec.16.3.10848.481-490
- [43] Tan, J., Zhang, W., Xia, A. (2013). Facile Synthesis of Inverse Spinel NiFe₂O₄ Nanocrystals and Their Superparamagnetic Properties. *Materials Research*, 16, 237-241. DOI: 10.1590/S1516-143920120050000157.
- [44] Zielińska-Jurek A., Bielan Z., Dudziak S., Wolak I., Sobczak Z., Klimczuk T., Nowaczyk G. and Hupka J. (2017). Design and Application of Magnetic Photocatalysts for Water Treatment. The Effect of Particle Charge on Surface Functionality. *Catalysts*, 7(360), 1-19. DOI: 10.3390/catal7120360
- [45] Das, H., Inukai, A., Debnath, N., Kawaguchi, T., Sakamoto, N., Hoque, S.M., Aono, H., Shinazaki, K., Suzuki, H., Wakiya, N. (2018). Influence of Crystallite on the Magnetic and Heat Generation Properties of La_{0.77}Sr_{0.23}MnO₃ Nanoparticles for Hyperthermia Applications. *Journal of Physics and Chemistry of Solids*, 112, 179-184. DOI: 10.1016/j.jpcs.2017.09.030.
- [46] Adeleke, J.T., Theivasanthi, T., Thirupathi, M., Swaminathan, M., Akomolafe, T., Alabi, A.B. (2018). Photocatalytic Degradation of Methylene Blue by

- ZnO/NiFe₂O₄ Nanoparticles. *Applied Surface Science*, 455, 195-200. DOI: 10.1016/j.apsusc.2018.05.184
- [47] Wu, L., Liu, X., Lv, G., Zhu, R., Tian, L., Liu, M., Li, Y., Rao, W., Liu, T. Liao L. (2021). Study on the Adsorption Properties of Methyl Orange by Natural One-dimensional Nano-mineral Materials with Different Structures. *Scientific Report*, 11, 1-11. DOI: 10.1038/s41598-021-90235-1
- [48] Niu, P. (2013). Photocatalytic Degradation of Methyl Orange in Aqueous TiO₂ Suspensions. *Asian Journal of Chemistry*, 25(2), 1103-1106. DOI: 10.14233/ajchem.2013.13539
- [49] Wang, F., Li, M., Yu, L., Sun, F., Wang, Z., Zhang, L., Zeng, H., Xu, X. (2017). Corn-like, Recoverable γ -Fe₂O₃@SiO₂@TiO₂ Photocatalyst Induced by Magnetic Dipole Interactions. *Scientific Reports*, 7, 1-10. DOI: 10.1038/s41598-017-07417-z
- [50] Alkaykh, S., Mbarek, A., Ali-Shattle, E.E. (2020). Photocatalytic Degradation of Methylene Blue Dye in Aqueous Solution by MnTiO₃ Nanoparticles under Sunlight Irradiation. *Heliyon*, 6, 1-6. DOI: 10.1016/j.heliyon.2020.e03663
- [51] Modirshahla, N., Behnajady, M.A., Rahbarfam, R., Hassani, A. (2012). Effects of Operational Parameters on Decolorization of C. I. Acid Red 88 by UV/H₂O₂ Process: Evaluation of Electrical Energy Consumption. *Clean – Soil, Air, Water*, 40(3), 298-302. DOI: 10.1002/clen.201000574
- [52] Zhao, H., Zhang, G., Chong, S., Zhang, N., Liu, Y. (2015). MnO₂/CeO₂ for Catalytic Ultrasonic Decolorization of Methyl Orange: Process parameters and mechanisms. *Ultrasonic Sonochemistry*, 27, 474-479. DOI: 10.1016/j.ultsonch.2015.06.009
- [53] Trablesi, H., Atheba, G.P., Hentati, O., Mariette, Y.D., Robert, D., Drogui, P., Ksibi, M. (2016). Solar Photocatalytic Decolorization and Degradation of Methyl Orange Using Supported TiO₂. *Journal of Advanced Oxidation Technologies*, 19(1), 79-84. DOI: 10.1515/jaots-2016-0110
- [54] Ammar, S.H., Elaibi, A.I., Mohamme, I.S. (2020). Core/shell Fe₃O₄@Al₂O₃-PMo Magnetic Nanocatalyst for Photocatalytic Degradation of Organic Pollutants in an Internal Loop Airlift Reactor. *Journal of Water Process Engineering*, 37, 1-11. DOI: 10.1016/j.jwpe.2020.101240
- [55] Pourzad, A., Sobhi, H.R., Behbahani, M., Esrafil, A., Kalantary, R.R., Kermani, M. (2020). Efficient Visible Light-induced Photocatalytic Removal of Paraquat

- using N-doped TiO₂@SiO₂@Fe₃O₄ Nanocomposite. *Journal of Molecular Liquids*, 299, 1-7. DOI: 10.1016/j.molliq.2019.112167
- [56] Li, Y., Li, X., Li, J., Yin, J. (2006). Photocatalytic Degradation of Methyl Orange by TiO₂-coated Activated Carbon and Kinetic Study. *Water Research*, 40, 1119-1126. DOI: 10.1016/j.watres.2005.12.042
- [57] Silva, da, C.G., Faria, J.L., (2003). Photochemical and Photocatalytic Degradation of an Azo Dye in Aqueous Solution by UV Irradiation. *Journal of Photochemistry and Photobiology A: Chemistry*, 155, 133-143. DOI: 10.1016/S1010-